Experimental Investigation on the Aerodynamics of a Bio-inspired Flexible Flapping Wing Micro Air Vehicle

Shuanghou Deng, Mustafa Percin, Bas van Oudheusden, Bart Remes and Hester Bijl

Faculty of Aerospace Engineering, Delft University of Technology, the Netherlands

ABSTRACT

An experimental investigation on a 10 cm bio-inspired flexible Flapping-Wing Micro Air Vehicle (FWMAV) was conducted in both hovering and forward-flight conditions with the objective to characterize its aerodynamic performance. The measurements in hovering conditions were performed with the particular objective to explore the effect of different wing configurations (i.e. different aspect ratios and wing flexibilities), whereas forward flight tests in a wind tunnel were carried out to assess the aerodynamic performance of the FWMAV as a function of flow speed, flapping frequency and body angle. The cyclic variation of forces (lift and thrust) generated as a result of the wing flapping was captured by means of a high-resolution force sensor, in combination with high-speed imaging to track the wing motion. Results of measurements in hover show that the flapping frequency, aspect ratio and wing flexibility have a crucial impact on the efficiency and the force generation during the flapping cycle. An estimated flight envelop for the MAV's operation is defined from the data obtained in the wind tunnel measurements. Furthermore, additional tests on several brushless DC motors provide a feasible option in future engine selection and design.

NOMENCLATURE

A	=	wake width of the flapping wings
f	=	flapping frequency
L	=	lift
P	=	power consumption
St	=	Strouhal number
T	=	thrust
t'	=	nondimensional stroke time
T/P	=	thrust to power ratio
U_∞	=	free-stream velocity
a	=	body angle of attack

1. INTRODUCTION

Recently, Micro Air Vehicles (MAVs) have increasingly become an active and highly integrated research topic at both scientific and technical level. The inherent small size and low cruise speed provide MAVs with a unique capability to perform specific civil and military tasks such as surveillance, assistance of indoor rescue and operation in dangerous environments without directly endangering a human operator [1]. Historically, three aeronautical concepts of MAVs have been considered, including fixed wing, rotary wing and flapping wing configurations [2]. When minimizing the size of MAVs to less than 15cm, fixed wing designs are increasingly affected by the deterioration in lift to drag ratio occurring in the low Reynolds number regime (typically $1\times10^3\sim1\times10^5$) [3]. For rotary wing MAVs, high noise, high rotor speeds, low energy efficiency and near-wall instability limit its potentials for indoor operations. On the other hand, flapping-wing MAV concepts, which are inspired from biological flyers have shown to be more efficient in terms of accomplishment of aforementioned tasks,

as they benefit from unconventional flapping-wing aerodynamic mechanisms, such as delayed stall [4], wake capture [5], and clap-and-fling [6].

A number of investigations have been reported that address flapping-wing aerodynamics in the specific context of FWMAVs. Aditya and Malolan [7] studied the effect of Strouhal number ($St = fA/U_\infty$) on the propulsive characteristics of an FWMAV. They found that there is a nominal dependence of propulsive characteristics on Strouhal number. They added that maximum propulsive force is attained for a narrow range of Strouhal numbers. Similar work was experimentally done by Muniappan et al [8] to study the effects of flapping frequency and amplitude on the lift production of an FWMAV. Their results revealed that lift increases with increasing flapping amplitude and flapping frequency and it decreases with increasing free-stream velocity. Moreover, they investigated the effects of wing aspect ratio, planform and flexibility on the aerodynamic force generation as a function of flapping frequency and free-stream velocity [9]. They found that higher aspect ratio wing generates noticeably more lift and slightly increased thrust. Besides, use of wings with more torsional flexibility can result in higher lift and thrust generation. Lin et al. [10] also measured the aerodynamic forces on a mechanical flapping system with flexible wings for various flapping frequencies, angles of attack and free-stream velocities. They concluded that the wing structural characteristics significantly affect the aerodynamic forces as a consequence of variation of wing deformation as a function of the flapping frequency. They reported that lift increases when increasing the flapping frequency at a certain flight speed. Hu et al. [11] conducted an experimental study to assess the aerodynamic performance of flexible membrane wings in flapping flight. They compared the performance of a rigid and two flexible wings in both flapping and soaring (non-flapping) flight conditions. They reported that flapping flight is considerably more beneficial in terms of force generation, particularly in the unsteady state regime with an advance ratio, which is the ratio of forward flight speed to wingtip velocity, being smaller than 1.0. They found that wing flexibility has a significant effect on the aerodynamic performance of the tested wings in both soaring and flapping flight conditions. Nakata et al [3] studied the flexible flapping wing aerodynamics on an X-wing flapper by combining wind tunnel measurements and a computational method. Wind tunnel measurements were performed to capture the wing deformations and forces generated during the flapping flight. Numerical simulations, on the other hand, were performed to provide a detailed and quantitative analysis of unsteady aerodynamic mechanisms. They underlined the effectiveness of the clap-and- fling mechanism as well as the importance of the wing flexibility. Mazaheri and Ebrahimi [12] realized a flapping-wing system to measure unsteady aerodynamic forces of the flapping wing motion for different flapping frequencies, angles of attack and free-stream velocities. They showed that thrust increases with increasing flapping frequency and decreases with increasing angle of attack and free-stream velocity. They also introduced a model to be used in the further design and optimization of the flapping wing.

Since 2005, the MAVlab at Delft University of Technology (DUT) has been engaged in the development and research of FWMAVs, investigating the related technologies regarding for example aerodynamics, flapping mechanisms, control electronics and flight autonomy. Three types of bio-inspired FWMAVs of different sizes have been developed over the past years: "DelFly I", "DelFly II" and "DelFly Micro" [13], the latter being the particular object of the present study. It is the DelFly philosophy to aim for reducing the size of the DelFly without sacrificing the flight performance and on-board functionality, as a result of which the smallest version flapper "DelFly Micro" was realized (see Figure 1), which has a maximum dimension of 10 cm and a fully-equipped weight of 3.07 grams. In each of the DelFly designs a so-called "X-Wing configuration" is employed, with two pairs of wings, mounted on each side of the fuselage and each wing pair flapping in counter-phase. This configuration provides a better flight stability compared to a single wing layout, while it further enhances force production through the clap-and-fling [6] effect. The desire to achieve a better understanding of the aerodynamic behaviour of these flapping MAVs, with the potential of further performance improvement, has formed the motivation of a series of experimental and computational studies on the "DelFly II" in particular [14-17] . These studies have provided valuable insight regarding the characterisation of the "DelFly II" design, but in view of its significantly larger dimensions (wing span 28 cm and 17 grams), the results may not be directly transferrable to the much smaller "DelFly Micro", which motivates the present study.

In this study, an experimental campaign has been conducted to characterise the "DelFly Micro", with specific focus on the forces produced during flapping motion in the hovering flight condition. The impact of wing flexibility has been assessed by testing different wing configurations, and an optimized

wing configuration has been experimentally selected. Wind-tunnel tests were carried out to provide an initial flight envelop of the FWMAV. Finally, several micro brushless motors (weight around half a gram) have been tested for performance and efficiency evaluation, in assistance of further design developments of the MAV.

2. EXPERIMENTAL MODEL AND SET-UP
2.1 MAV Degisn
"DelFly Micro" prototype which was designed and built in the Micro Air Vehicle Laboratory (MAVLab) of DUT is illustrated in Figure 1. It has a flat wing span of 10 cm, with an aspect ratio of about 3.2. The wing's planform was directly downscaled from the "DelFly II", and is constructed out of a Mylar membrane with carbon fiber stiffener rods. A frosted 3D printed hinge system drives the flapping motion of the two pairs of wings and determines its kinematics. Force-enhancing clap-and-fling events [18] occurs three times during each flapping cycle: twice on both sides at the stroke reversal of each wing pair, and additionally once at the top between the upper wings of each wing pair. The latter is a result of the large stroke amplitude of 60º for each wing, which forms a distinction from the bigger version 'DelFly II', where this does not occur. It should be noted that the aerodynamic behaviour of the upper wings is, hence, not entirely the mirrored version of the lower wings, due to this top clap-and-fling event. The gearbox is milled from an in-house made carbon-balsa-carbon sandwich structure to ensure light weight and strong structure. A brushed DC motor drives the two-stage gear system with a reduction ratio of 33.3 that runs the wing pairs in flapping motion. Two 180 Ohm magnetic actuators with a weight of 0.12 g each are utilized to actuate a rudder and an elevator that are built on the tail. The control of the actuators and brushed DC motor is achieved via a 4-channel receiver and Radio Control Transmitter. The front-mounted camera and the transmitter make the "DelFly Micro" the smallest ornithopter with on-board camera in the world. A 50 mAh lithium polymer battery can enable "DelFly Micro" for a 3 minutes flight duration and 50 meters range. With all the parts mounted, "DelFly Micro" only weights 3.07 gram.

It is realized from free flight test that the small brushed DC motor (Ø = 4 mm) equipped on "DelFly Micro" woule be easily overheated during the flying, which inspires us to search more powerful and efficient micro brushless motors in future optimizing design. In the measurements, the small motor of the flying MAV was replaced by a relative bigger brushed DC motor (Ø = 7 mm) to enforce a longer life time, thus facilitating the ease of measurement. Note that this big brushed DC motor weights around 2.78 grams which cannot be used on the flying "Delfly Micro" due to its considerable weight.
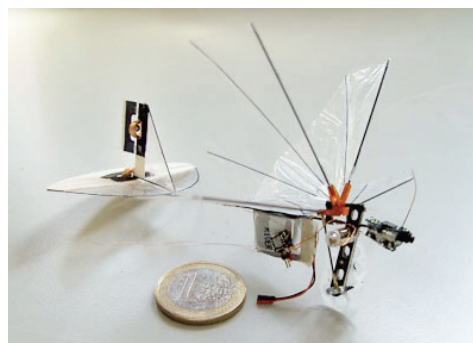

Figure 1. "DelFly Micro" prototype.

2.2 Experimental Set-Up
Experiments were performed in a low-speed wind tunnel at the Aerodynamic Laboratory of DUT. The wind tunnel has an open test section with cross-section dimensions of 0.6 m × 0.6 m. In-hover measurements were performed at zero free-stream velocity while for forward-flight measurements, the free-stream velocity was set to 2, 3 and 4 m/s accurately by use of a hot-wire anemometer. The corresponding Reynolds numbers based on the free-stream velocity and mean chord length range from 4×10^3 to 8×10^3. The flapping frequency of the "DelFly Micro" was determined by means of a photodiode sensor positioned around the main gear, and the tested frequencies range from 20 Hz to 35 Hz, with an increment of 5 Hz.

Six components of forces and moments were captured by use of an ATI Nano17 Titanium force sensor that is attached to a balance mechanism. It is recently the smallest 6-axis sensor for commercial use and can resolve down to 0.149 gram-force without filtering. The FWMAV was mounted on the force sensor via a custom design clamp as in Figure 2 (a). There are two DC motors coupled with the kinematic system of the balance strut to change the pitch angle (from -15° to 35°) and the yaw angle of the mounted model. By use of the pitch motor, forward flight tests were performed at the body angles of 20°, 30° and 40°. Figure 2 (b) shows the schematics of the lift and thrust correspond to the body axis reference frame.

A Photron Fastcam SA 1.1 camera was placed in front of the experimental model to record the spatial positions of the leading edges of both upper and lower wings to determine the stroke angle during the flapping cycle, which then can be related to the acquired forces. A series of 1000 images were recorded during each test with a recording rate of 3000 Hz to ensure that at least 10 flapping cycles are captured even at the maximum flapping frequency of 35 Hz. Recorded images were pre-processed to improve the contrast and have a clear image of the leading edges using built-in functions of MATLAB. Then a Hough transform was performed on the pre-processed images in order to detect the leading edges and to calculate the stroke angles.

An in-house programmed Field-Programmable Gate Array (FPGA) system of National Instruments was used for both data acquisition and synchronization of force measurements and high speed imaging with the flapping motion. In addition to the six components of forces and moments, voltage and current directly fed to the brushed motor were also acquired simultaneously which allows calculation of power consumption of the motors throughout the flapping cycle. A data acquisition rate of 12.5 kHz was used in all measurements.

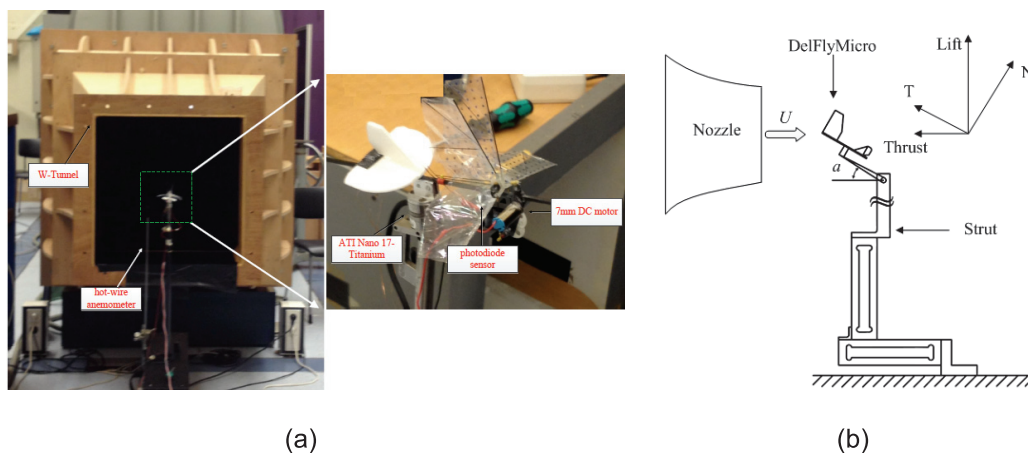(a)   (b)

Figure 2. Experimental set-up: (a) 'Delfly Micro' mounted on force balance; (b) Experimental apparatus and the force definition.

The raw data output was filtered by a Chebyshev II low-pass filter with -80 dB attenuation of the stopband in MATLAB. A forward-backward filtering technique was implemented by use of 'filtfilt' function of MATLAB in order to prevent time-shift of the data. Selection of the cut-off frequency is troublesome as the sensor captures aerodynamic forces as well as inertial forces and mechanical vibrations of the DelFly components. In the sense of analysis of the mean forces, it is plausible to assume that inertial force generated by the wing during upstroke is largely cancelled out by that during downstroke which results in a time-averaged value of zero [19]. Nevertheless, proper analysis of time history of aerodynamic forces requires more elaborate investigation to determine the cut-off frequency such that all inertial effects and mechanical vibrations are eliminated. Therefore, in-vacuum tests were performed at an ambient pressure of 1 mbar, in order to provide information about the distinction between the aerodynamic and inertial contributions to the forces generated by the flapping motion.

Power spectral densities of in-air and in-vacuum measurements of the thrust component are compared in Figure 3 for the standard DelFly wings with a Mylar thickness of 2 µm, at a flapping frequency of 30 Hz. A part of the spectrum up to 200 Hz is represented for a better visualization of

relevant force harmonics. It is clear that the second, third and fourth harmonics of the flapping motion have dramatically higher amplitude in air than that in vacuum conditions, which strongly suggests that they can be attributed to the aerodynamic forces. The second harmonic has the strongest amplitude in the aerodynamic force, as during every flapping cycle peaks occur at both instroke and outstroke. The first harmonic, which is essentially the flapping frequency, has comparable amplitudes in both cases. It can be attributed to an asymmetric vibration of a DelFly component at the driving flapping frequency. Nevertheless, comparison of air and vacuum conditions still reveals aerodynamic contribution in the first harmonic. As a result of a finite element analysis in CATIA V5, the small peak around 50 Hz is found to correspond to the frequency of the first structural mode of the support which was used to mount the model in the vacuum test setup. The amplitudes of fifth and sixth harmonics are higher in vacuum conditions while they are damped in the case of flapping in air. This suggests that these peaks likely correspond to wing structural mode excitations. As a result, it was decided to use a low-pass filter with a cut-off frequency that eliminates wing structural modes and keeps the first four harmonics for the analysis of the aerodynamic force data.
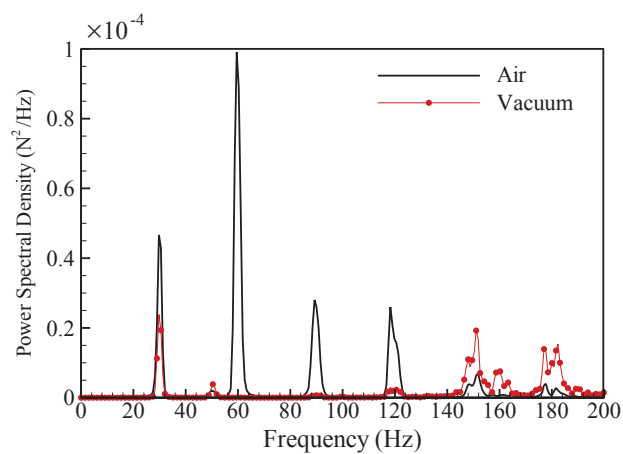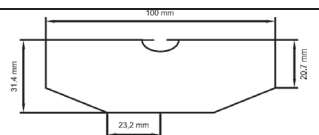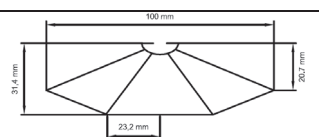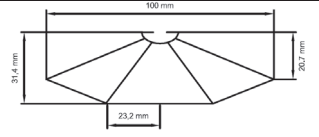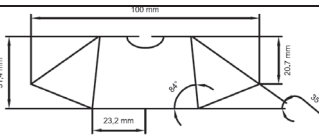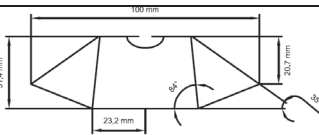

Figure 3. Power spectrum for thrust in air and vacuum, f = 30 Hz.

2.3 Tested Wing Construction

All the wings in the tests were manufactured by using a pre-milled vacuum table to guarantee a uniform tension of the membrane foil. Six wings with different flexibility were designed by varying membrane thickness and stiffeners orientation, as depicted in Table 1. A wing nomenclature has been adopted in

Table 1 Tested Wings

Name	Thickness (μm)	Layout	Mass (mg)
Clear 2	2		32
Clear 5	5		50
Std 2	2		58
Std 5	5		66
Std 10	10		75
RadStiff 2	2		54

which the number in the name of the wings represents the membrane thickness in μm. 'Clean' indicates the wings without stiffeners; 'Std' is the standard wing which is downscaled from the current 'DelFly II', while 'RadStiff' represents the wing that is stiffed with normal radial orientation. All the wings used in the testing were made on the same vacuum table at the same time to minimize structural differences.

3. RESULTS AND DISCUSSION
3.1 Time History of the Force

First, temporal evolutions of thrust for the wing Std 2 are compared for different flapping frequencies. Then a comparison is performed for different wing configurations at a flapping frequency of 20 Hz. The instaneous historical force synchronized with the flapping stroke angles versus non-dimensional time are plotted in Figure 4. Solid and dashed lines represent the wing motion for the upper and lower wings, respectively. It can be seen that the sinusoid flapping stoke angle ranges from 0° to 120°. Force results are given in Figure 4 (a) for three different frequencies. The force production displays two peaks of different magnitude, the first occurring after the onset of outstroke and the second after the beginning of the instroke. The flapping frequency significantly influences the force production, in the sense that flapping faster yields a considerable increase in force generation at peaks regimes. When comparing the force generation by varying the flexibility of the wing, through a change of the membrane thickness, the more rigid wing marginally increases the force generation compared to the flexible wing, according to Figure (b).
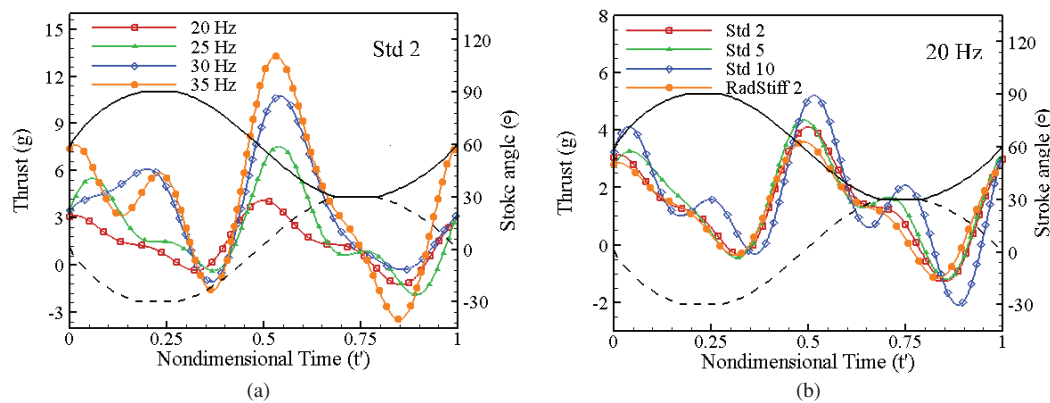

Figure 4. Thrust (left Y axis) and wing stroke angle (right Y axis) variation vs. nondimensional time, t': (a) Effect of flapping frequency for Std 2 wing; (b) Effect of membrane thickness and stiffeners orientation at f=20 Hz.

3.2 Effect of Flexibility

As shown in Figure 5, mean thrust generated as a result of the flapping motion has almost a linear dependence on the flapping frequency for all of the wings. On the other hand, the power consumption increases more than linearly with the flapping frequency. As a result, the efficiency (thrust to power ratio) decreases with frequency, for all wings. The clean wing configuration (i.e., without stiffeners) requires the smallest power input when compared with the stiffened wings. However, the low thrust generated by the clean wing results in an inefficient configuration in view of the thrust to power ratio, see in Figure 5 (c). For the wings with stiffeners, thrust production also increases with increasing Mylar foil thickness at a given flapping frequency. Wing Std 2 has a lower thrust production as may be expected from the increased amount of flexibility. Figure 5 (b) illustrates that the more rigid wing required more power input for a given frequency. From Figure 5 (c), it follows that all the stiffened wings have better thrust to power ratio than the clean wings, and that Wing Std 2 possesses the best performance. Wing RadStiff 10 displays the original wing stiffener configuration that has been used on the "Delfly Micro" in the past, and which was also examined for comparison. One can see that this wing configuration generates less thrust than the other stiffened wings. Meanwhile, it is more power consuming and a poor T/P performance of the RadStiff 10 wing results, as can be seen in Figure 5 (c). Overall, it is clear that force production and power consumption increases with increasing stiffness of the wing. The standard wing
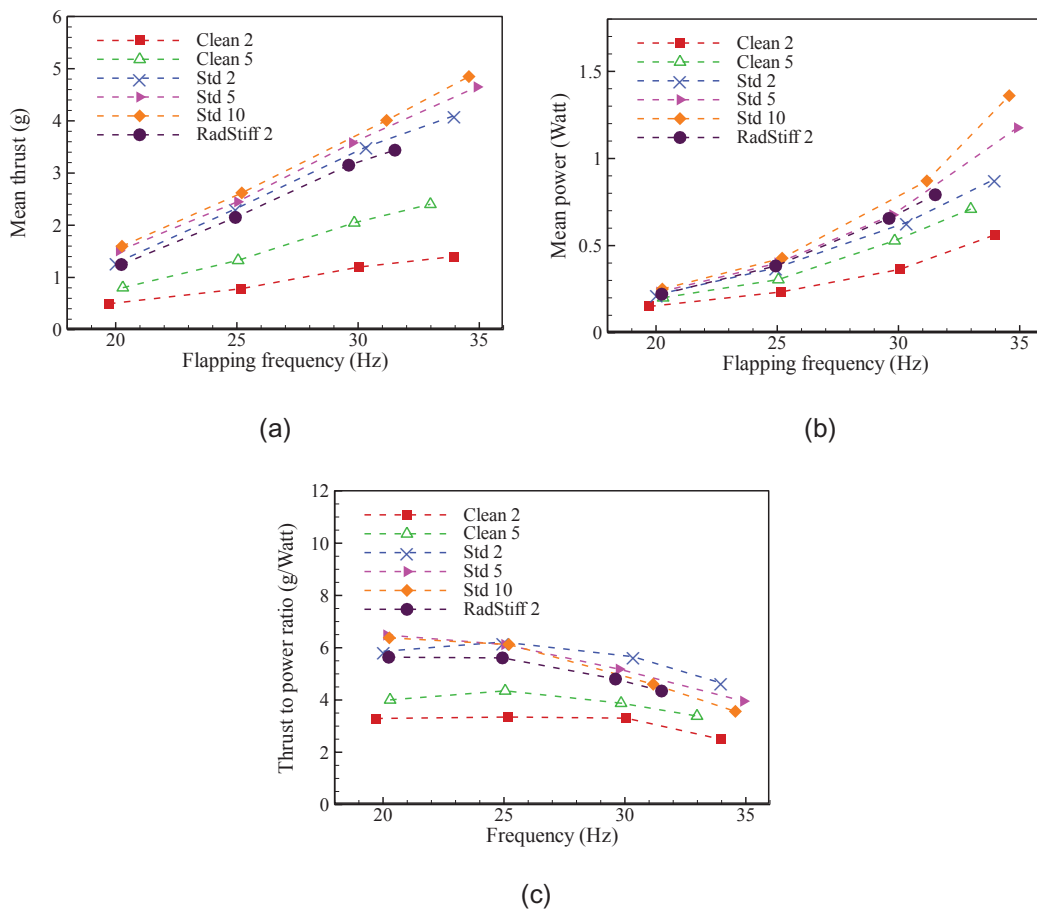
(a)

(b)

(c)

Figure 5. Performance plots for wings with different flexibility; (a) Mean thrust. (b) Mean power consumption. (c) Thrust to power consumption ratio.

built with a 2 µm foil displays the best performance, in terms of the highest thrust to power ratio within the enveloped flapping-frequency range of the "DelFly Micro" between 25 Hz and 35 Hz. Note that the thrust generated around 30 Hz is about 3 grams, which is equal to the total weight of the "DelFly Micro". That means the "DelFly Micro" is potentially able to hover, according to these measurements.

3.3 Effect of Aspect Ratio

To evaluate the impact of wing span (aspect ratio) of the wing, tests were conducted on three sets of flapping wings with different span lengths, namely 80 mm, 100 mm and 120 mm, respectively, as illustrated in Figure 6 (a). The wings are only scaled in the spanwise direction, while the mean chord length is kept constant, implying that when changing the wing span, the wing surface area is altered correspondingly. Figure 6 (b) plots the mean thrust generated by the different wings, and shows that increasing the wing span results in a significant increase in thrust generation. By increasing the span length at 2 cm per step, the thrust increases more than proportionally. Despite the fact that for a given flapping frequency, the wing with a longer span length consumes more power (Figure 6 (c)), it still has a better thrust to power ratio (Figure 6 (d)).

3.4 Wind Tunnel Tests

Where in the previous section the flapping performance for the 'DelFly Micro' under hovering conditions was investigated, the present section will address the situation with an incoming flow, representing the forward flight regime. The calibrated wind speed U_∞ is set at 2 m/s, 3 m/s and 4 m/s. For each velocity, the angle of attack was varied from 20° to 40° with an increment of 10°. Both lift and thrust were measured during the tests. Note that the forces measured on the force sensor were
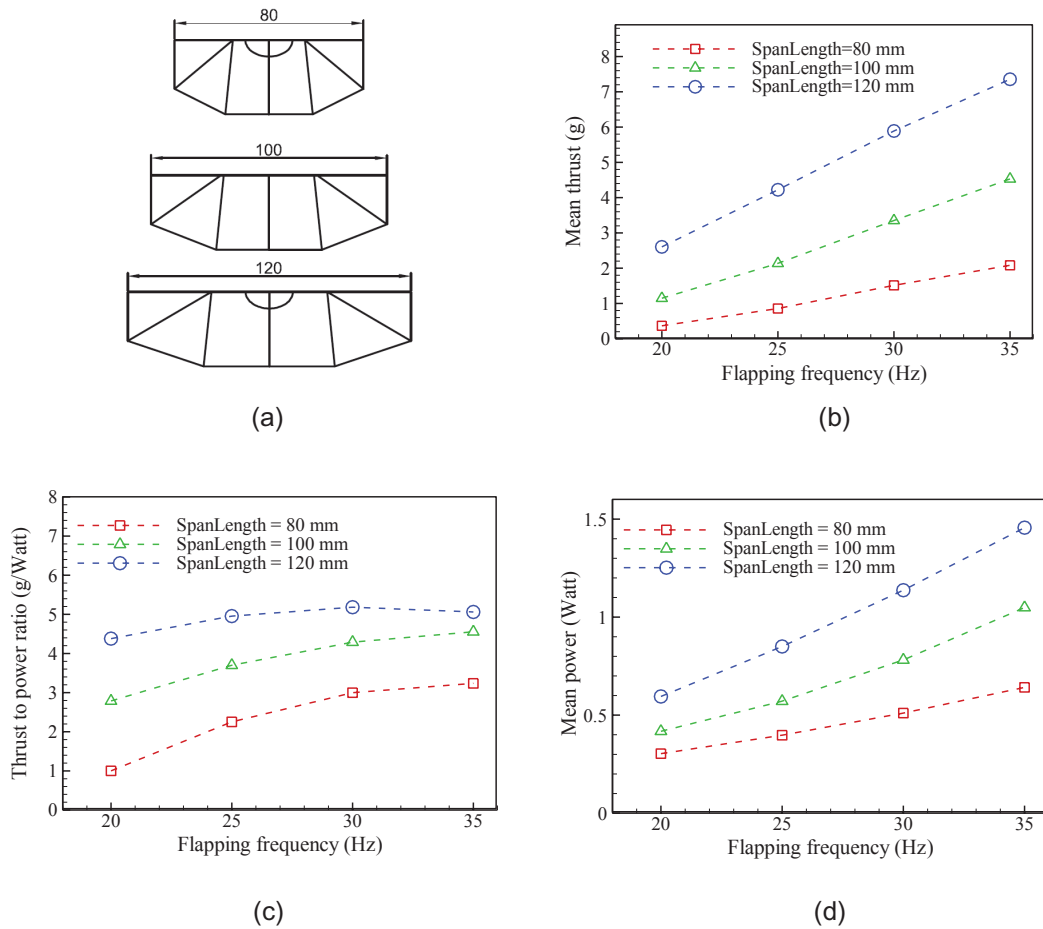
Figure 6. Aerodynamic performance of different aspect ratio wings: (a) Wing schematics with different aspect ratio; (b) Thrust production vs. frequency; (c) Mean power vs. frequency; (d) Thrust to power ratio vs. frequency.

actually obtained as the normal and tangent forces respective to the (body-fixed) balance plane, from which lift and thrust were computed in the free stream-aligned coordinate frame, see in Figure 2 (b).

Figure 7 shows the lift versus thrust for varying flapping frequency and free stream velocity. The origin point (indicated by the solid circle dot) of the inner coordinate system represents the equilibrium flight point, where the generated average lift equals the weight (3.07 gram) of the MAV and net average thrust is zero. The first quadrant of the inner coordinate system can, hence, be viewed as the flight operation region where net lift and thrust are available. For the investigated range of flapping frequency and angle of attack, some points fall within the flight operation region for U_{∞} = 2 m/s and 3 m/s, but this is not the case for U_{∞} = 4 m/s. This suggests that the MAV may not be able to fly at a speed of 4 m/s or higher. Moreover, the level flight point in Figure 7 (a) indicates that "DelFly Micro" can fly at 2 m/s when f = 28 Hz and α = 36° angle of attack. By increasing the frequency to 34 Hz "DelFly Micro" a flight speed of 3 m/s can be achieved, with α = 25°, as depicted in Figure 7 (b).

3.5 Motor Study

The "DelFly Micro" is currently powered by a small brushed DC motor and this type of motor has to be dramatically overloaded for providing a 30 Hz flapping frequency or even more. It is foreseen to use a powerful brushless motor to solve the overheat problem in an improved design. However, the small carrying capacity of the MAV critically limits the permissible motor weight. After a series propeller-based tests, three candidate motors were identified, see in Table 2. The 'RCmotor' is custom made by www.microbrushless.com, while the CO2 motors are available from www.gasparin.cz.
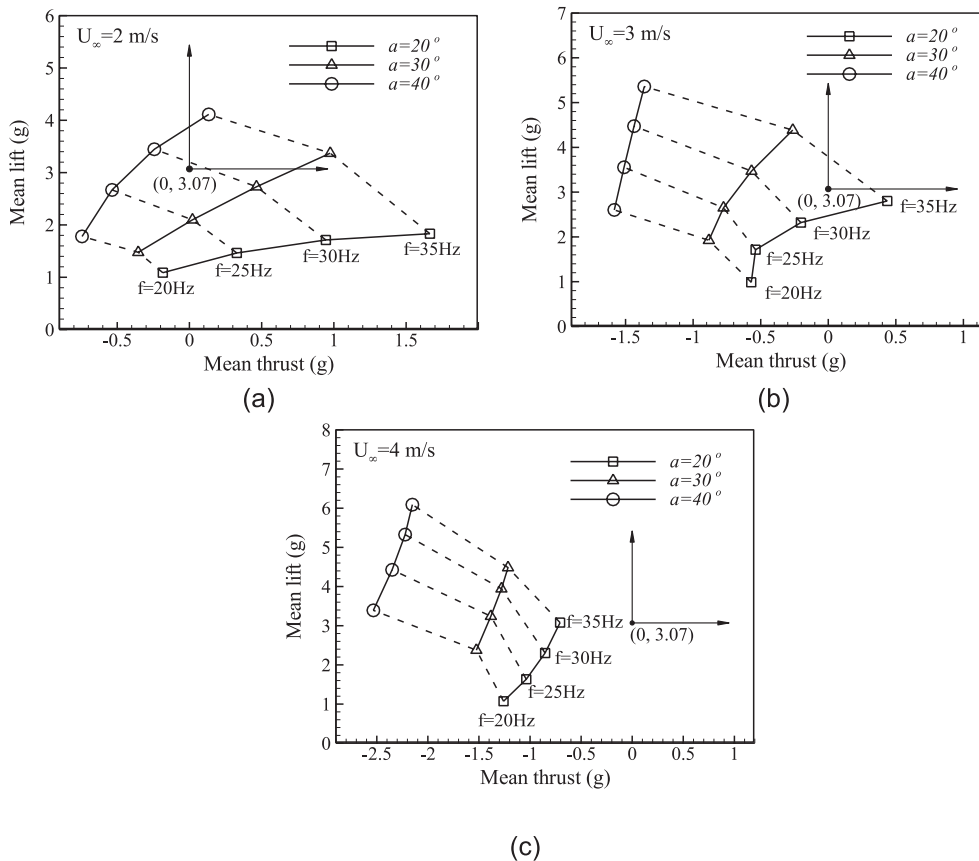
(a)

(b)

(c)

Figure 7. Lift and Thrust with varying incoming flow velocity: (a) U^{∞} = 2 m/s; (b) U_{∞} = 3 m/s; (c) U_{∞} = 4 m/s.

Table 2 Tested motors

Motor	Weight, g	Diameter, mm
RCmotor	0.6	10
CO2_500	0.5	8.8
CO2_600	0.6	8.8

The motors were mounted on the MAV model with the same mechanical system, and controlled by an in-house built control board. Std 2 wings were used in test. The thrust to power ratio was considered again as the characterising parameter in evaluating the performance of the motors. Figure 8 depicts the operating performance of the three tested brushless motors, from which it can be concluded that the 'RCmotor' possesses the best performance.
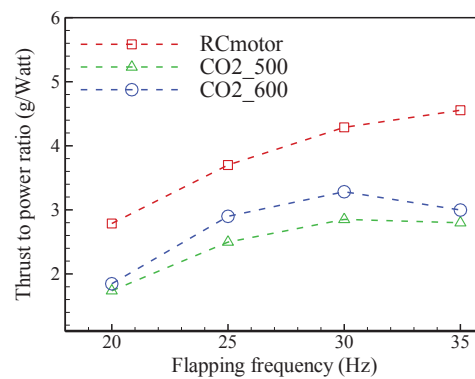
Figure 8. Performance of the motors.

4. CONCLUSIONS

Experiments have been conducted to investigate the aerodynamic performance of a bio-inspired flexible flapping-wing MAV, the "DelFly Micro", which has a flat wing span of 10 cm and a weight of 3 grams. Particular points of attention in the study were the time-variation of the forces over the flapping period, and the effect of wing layout and flexibility on the aerodynamic performance. Wind tunnel tests have also been carried out to define an initial flight envelop of the MAV. Finally, additional motor tests were performed to select a powerful and light engine to be used in future design developments.

In summary, the following conclusions can be derived from this study:

1) The flapping frequency crucially influences the force production, where a higher frequency will result in a considerable increase in force. Two force peaks were revealed within one flapping cycle which are different in amplitude. The smaller one locates at the end of fling and the higher one peaks after the clap has started.

2) The flexibility of the wing significantly influences the flapping performance. More rigid wings can produce higher forces during flapping, however, they are also more energy consuming. The Std 2 wing possesses the best performance of the investigated wings, with slightly lower thrust compared to the wings made from 5 µm and 10 µm thickness membranes. Wings with higher aspect ratio (larger span) can substantially increase the forces.

3) Wind tunnel tests define the initial flight envelop, and suggest that the 'DelFly Micro' can theoretically achieve a level flight up to at least 3 m/s, with 34 Hz flapping frequency and 25° angle of attack.

4) A brushless motor has been tested and selected as most promising engine for the next generation MAV.

ACKNOWLEDGMENTS

REFERENCES

[1]   I. Chopre, *Hovering Micro Air Vehicles: Challenges and Opportunities*, *Proceedings of the American Helicopter Society Specialists*, VA, 2007.

[2]   T.J. Mueller, *Fixed and Flapping Wing Aerodynamic for Micro Air Vehicle Applications*, *Progress in Astronautics and Aeronautics*.2001, 195, 61-81.

[3]   T. Nakata, H. Liu, Y. Tanaka, N. Nishihashi, X. Wang, and A. Sato, Aerodynamics of a Bio-inspired Flexible Flapping-Wing Micro Air Vehicle, *Bioinspiration &Biomimetics*, 2011, 6(4), 1-11.

[4]   H.M. Dickinson, The Effects of Wing Rotation on Unsteady Aerodynamic Performance at Low Reynolds Numbers, *Journal of Experimental Biology*, 1994, 192(1), 179-206.

[5]   C.P. Ellington, C. Van De Berg, A.P. Willmott, and A.L.R. Thomas, Leading-Edge Vortices in Insect Flight, *Nature*, 1996, 384: 626-30.

[6]   T. Weis Fogh, Quick Estimates of Flight Fitness in Hovering Animals, Including Novel Mechanisms for Lift Production, *Journal of Experimental Biology*, 1973, 59, 169-230.

[7]   K. Aditya, and V. Malolan, Investigation of Strouhal Number Effect on Flapping Wing Micro Air Vehicle, *AIAA Paper*, 2011, 486.

[8]   A. Muniappan, V. Duriyanandhan, and V. Baskar, Lift Characteristics of the Flapping Wing Micro Air Vehicle, *AIAA Paper*, 2004, 6331.

[9]   A. Muniappan, V. Baskar, and V. Duriyanandhan, Lift and Thrust Characteristics of Flapping Wing Micro Air Vehicle (MAV), *AIAA Paper*, 2005, 1055.

[10] C.S. Lin, C. Hwu, and W.B. Young, The Thrust and Lift of an Ornithopter's Membrane Wings with Simple Flapping Motion, *Aerospace Science and Technology*, 2005, 10(2), 111-19.

[11] H. Hu, G.A. Kumar, G. Abate, and R. Albertani, An Experimental Investigation on the Aerodynamic Performances of Flexible Membrane Wings in Flapping Flight, *Aerospace Science and Technology*, 2010, 14(8), 575-86.

[12] K. Mazaheri, and A. Ebrahimi, Experimental Investigation on Aerodynamic Performance of a Flapping Wing Vehicle in Forward Flight, *Journal of Fluids and Structures*, 2011, 27(4), 586-95.

[13] www.delfly.nl.

[14] E. De Croon et al, Design, aerodynamics and autonomy of the DelFly, *Bioinspiration &Biomimetics*, 2011, 7(2), 1-16.

[15] M. Percin, Y. Hu, B.W. van Oudheusden, B.W. Remes, and F. Scarano, Wing Flexibility Effects in Clap-and-Fling, *International Journal of Micro Air Vehicles*, 2011, 3(4), 217-27.

[16] W.B. Tay, H. Bijl, and B.W. van Oudheusden, Analysis of Biplane Flapping Flight with Tail, *AIAA Paper*, 2012, 2968.

[17] M.E.K. De Clercq, R. De Kat, B.W. Remes, B.W. van Oudheusden, and H. Bijl, *Flow Visualization and Force Measurements on a Hovering Flapping-Wing MAV 'Delfly II'*, *AIAA Paper*, 2009, 4035.

[18] L.N. Bradshaw, and D. Lentink, Aerodynamic and Structural Dynamic Identification of a Flapping Wing Micro Air Vehicle, *AIAA Paper*, 2008, 6248

[19] Y. Hong, and A. Altman, Lift from Spanwise Flow in Simple Flapping Wings, *Journal of Aircraft*, 2008, 45(4), 1206-16.